

SIXTH EUROPEAN ROTORCRAFT AND POWERED LIFT AIRCRAFT FORUM

PAPER NO. 18

DEVELOPMENT OF ANTIRESONANCE FORCE ISOLATORS FOR
HELICOPTER VIBRATION REDUCTION

D. Braun
Messerschmitt-Bölkow-Blohm GmbH
Munich, Germany

September 16-19, 1980
Bristol, England

THE UNIVERSITY, BRISTOL, BS8 1HR, ENGLAND

DEVELOPMENT OF ANTIRESONANCE FORCE ISOLATORS FOR HELICOPTER VIBRATION REDUCTION

D. Braun

Messerschmitt-Bölkow-Blohm GmbH
Munich, Germany

Abstract

One method of reduction of the rotor induced cabin vibrations consists of separating the helicopter fuselage dynamically from the rotor-transmission unit by use of convenient isolator elements. An example of such a device is one which is essentially formed by the parallel connection of a spring and a passive force generator, and which works according to the well known antiresonance principle.

This paper deals with the development of two different types of uniaxial antiresonance force isolators. They are suitably arranged at several points, in different operating directions, as connecting members between gearbox and fuselage, to obtain multiaxis vibration isolation. One of these isolators is a conventional model; the other one is a novel type distinguished by very low inherent damping, total symmetrical arrangement of all components, and simple wear-resistant design. Sufficiently exact theoretical descriptions are developed for both isolator types.

The effectiveness of the presented force isolators is tested by use of an uniaxial functional model by which the free-free condition of the flying helicopter can be simulated in the vertical direction. Good agreement is achieved between theoretical and experimental results. In particular with the novel version excellent isolation efficiency is obtained.

Nomenclature

A_P	effective cross-sectional area of the primary bellows, m^2
A_S	effective cross-sectional area of the secondary bellows, m^2
c_D	damping coefficient of the isolator spring, kg/s
c_F	} radial damping coefficients of the pendulum bearings, kg/s
c_R	
c_S	axial damping coefficient of the secondary bellows, kg/s
c_T	torsional damping coefficient of the pendulum bearings, Nms
c_T^*	abbreviation, $= 2c_T/e^2$
c_v	volume damping coefficient of the bellows system, kg/s
c_z	damping coefficient of the additional spring, kg/s
[C]	damping matrix
e	distance between the pendulum bearings, m

f frequency, Hz
 F_R rotor excitation force, N
 $\{F_R\}$ excitation vector
 F_{R0} amplitude of rotor excitation, N
 I_D moment of inertia of the pendulum bar, kgm^2
 I_D^* abbreviation, $= I_D/e^2$
 k_D stiffness of the isolator spring, N/m
 k_F } radial stiffnesses of the pendulum bearings, N/m
 k_R }
 k_p } axial stiffnesses of the bellows, N/m
 k_s }
 k_T torsional stiffness of the pendulum bearings, Nm
 k_T^* abbreviation, $= 2k_T/e^2$
 k_v volume stiffness of the bellows system, N/m
 k_z stiffness of the additional spring, N/m
 k_{tot} total isolator stiffness, N/m
 $[K]$ stiffness matrix
 $[M]$ inertia matrix
 M_D pendulum mass, kg
 M_F fuselage mass, kg
 M_R rotor-transmission mass, kg
 Δp dynamical pressure in the fluid, bar
 Q_A ratio of the effective cross-sectional areas of the bellows,
 $= A_p/A_s$
 Q_R lever ratio of the mechanical pendulum, $= R_D/e$
 R_D length of the pendulum bar, m
 t time, s
 $\{z\}$ displacement vector
 Δz dynamical relative displacement between fuselage and rotor-
transmission mass, mm
 z_D absolute coordinate for the pendulum weight
 z_F absolute coordinate for the fuselage mass
 z_R absolute coordinate for the rotor transmission mass
 Φ_D auxiliary angle coordinate for the pendulum bar
 ζ_{tot} damping ratio of the total isolator referred to the rotor
transmission mass
 ω excitation frequency, 1/s
 ω_a tuning frequency, 1/s
 Ω rotary frequency of the main rotor, 1/s

1. Introduction

During the last decade, remarkable progress with regard to performance, in particular of light and medium weight helicopters, has been obtained. Novel rotor systems, which not only permit higher speeds but also considerably improve maneuverability, have contributed to essentially extend the range of mission of such helicopters. The increasing usage of helicopters for accident rescue, the demand for installation of highly sensitive instruments in the helicopter, and last but not least the hope of the helicopter industry to be able to enter the market of business airplanes, have led to intensify research on one of the main outstanding problems of the helicopter: vibration reduction.

The main excitation has its origin in the rotor and is conditional upon the helicopter flight principle itself. The nonuniform air flow through the main rotor in forward flight causes periodically variable air loads on the rotor blades leading to sinusoidal excitation forces and moments at the rotor hub. These rotor vibratory loads consist of so-called "number-of-blades" harmonic components with the frequencies $n\Omega$, $2n\Omega$, etc., where n is the number of rotor blades and Ω the rotor rotational speed. In general, the $n\Omega$ harmonic is the dominant helicopter excitation.

A method of reducing rotor induced cabin vibration is rotor isolation by using specific force isolators as connecting members between rotor-transmission unit and fuselage. The passive antiresonance force isolator represents an attractive compromise between effectiveness and technical resources. Several rotor isolation systems with such isolator elements have been proposed or flown [1-5]. The purpose of the present paper is to demonstrate the development of two different types of passive antiresonance force isolators providing an effective multiaxis nodal isolation system for hingeless rotor helicopters.

2. The isolation system

The MBB concept of a passive nodal vibration isolation system for helicopters is as follows: the helicopter fuselage is separated dynamically from the rotor-transmission unit by use of uniaxial antiresonance force isolators. They are arranged at several points, in different operating directions, as connecting members between gearbox and fuselage to obtain multiaxis vibration isolation. The number of isolator elements depends on the number of the required isolation axes. From the theoretical point of view this kind of isolation is independent of the fuselage elasticity. For a certain frequency, forces which have their origins in dynamic rotor loads, are eliminated locally by inertia forces. In Fig. 1 the schematic view of a five-axes vibration isolation system, consisting of six force isolator elements, is shown. This arrangement allows the isolation of longitudinal, lateral, vertical excitation forces and of roll and pitch excitation moments. To guarantee freedom of movement of the rotor-transmission unit normal to the operating axes of the particular force isolators, it is necessary to join the elements to the fuselage and the gearbox respectively by ideal spherical bearings. To avoid any play and any friction in the transmission suspension, it is useful to represent the ideal spherical bearings by so-called quasi-hinges, which have to be "soft" compared with the axial stiffness of the isolator springs (Damping

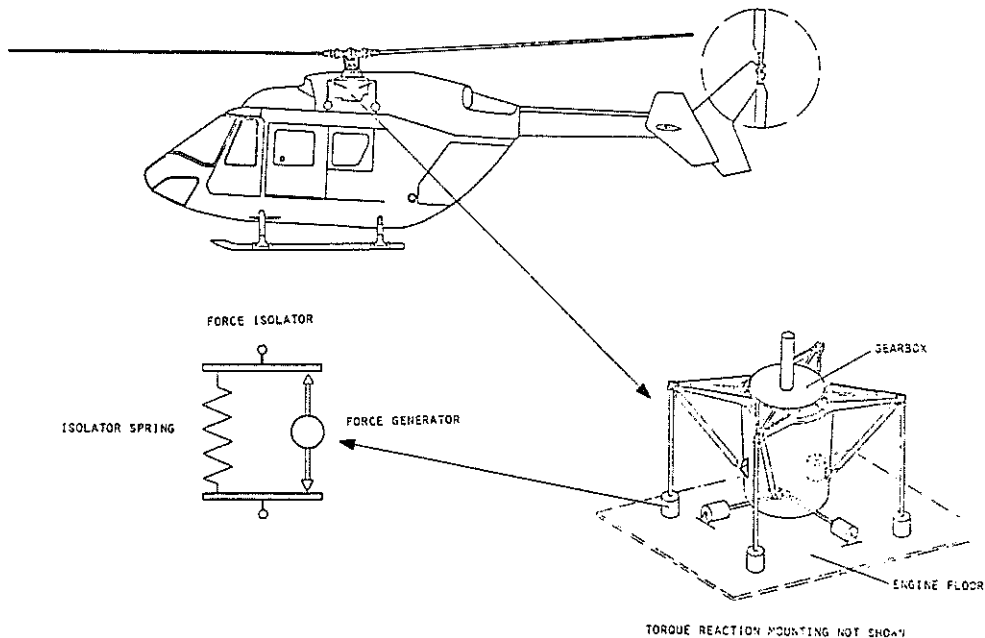


Figure 1: Schematic view of a five-axes nodal vibration isolation system and secondary springs in the transmission suspension impair the efficiency of the isolation system.)

The use of uniaxial isolator elements offers the following advantages:

- mechanically simple construction of the isolator elements
- well-defined separation of the load paths
- universal applicability to different types of helicopters
- mechanical assembly technique for creating isolation systems with one or more isolation axes.

3. Principle of operation

The present paper outlines the development of local uniaxial force isolators which are part of a passive nodal vibration isolation system. The single isolator is essentially formed by the parallel arrangement of a spring and a passive force generator, and operates according to the antiresonance principle. The method of operation is such, that for a certain excitation frequency (antiresonance frequency) the dynamic part of the spring force and the dynamic force, produced in the force generator by the relative movement between fuselage and rotor-transmission unit, are opposite and equal at the fuselage side attachment point of the isolator element.

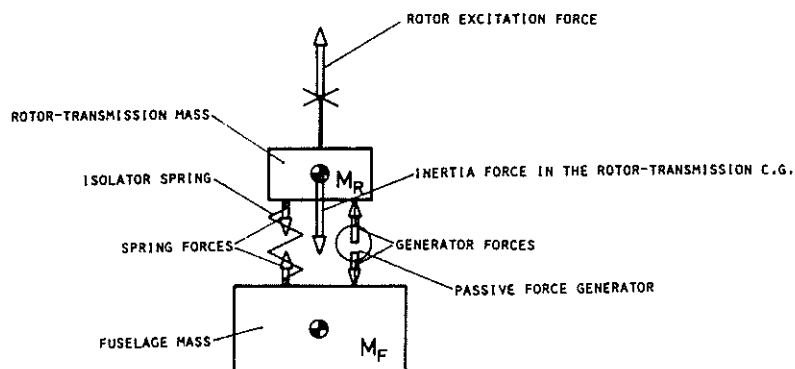


Figure 2: Antiresonance force isolator: dynamic force balance in the isolation case

The rotor excitation forces and moments are compensated by inertia forces and moments of the rotor-transmission unit itself. In Fig. 2 the dynamic force balance in the isolation case is illustrated for a simple one-degree-of-freedom system.

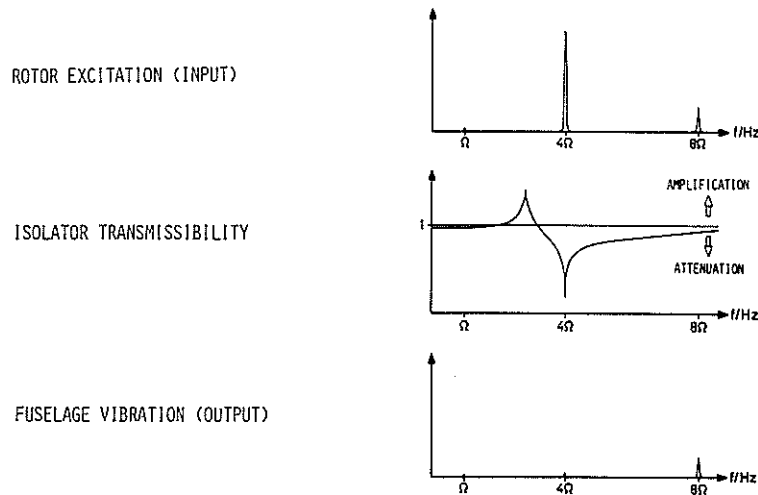


Figure 3: Mode of action of the antiresonance force isolator

The mode of action is explained in Fig. 3. The rotor excitation spectrum (input) is reduced, by the isolator transmissibility, to the fuselage vibration spectrum (output). Thereby, the isolator may be considered as a notch filter for the main disturbing frequencies.

Two different types of uniaxial antiresonance force isolators have been developed in the MBB ARIS program (Anti-Resonance Isolation System). One of these isolator elements is fitted out with a conventional force generator consisting of a mechanically driven pendulum. The other one is a novel type of antiresonance isolator equipped with an hydraulic passive force generator.

4. Isolator with mechanical force generator

The antiresonance isolator with a mechanically driven pendulum is in principle well known [1]. However, only experimental versions of such isolator types have been flown until now [2-4]. The construction design and the schematic view of the mechanical isolator, developed in the ARIS program, is shown in Fig. 4. It is one of four vertical isolator elements qualified for installation in the BK 117 helicopter. The essential construction aims were:

- transmission of the static rotor loads not by the hinges of the isolator pendulum, but by special structural elements
- use of low friction pendulum bearings, free from play
- use of connecting members between isolator and gearbox which approach the behaviour of ideal pinned joints
- high life time and low damping by use only of frictionless quasi-hinges

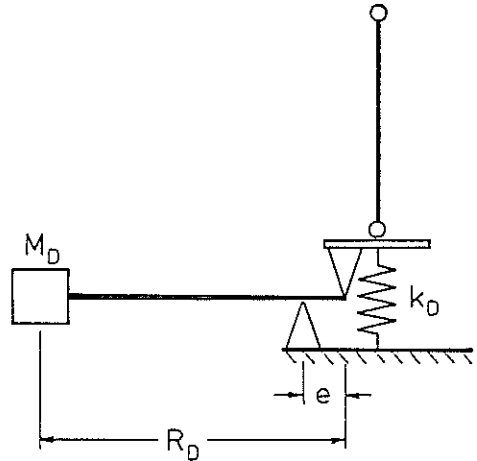
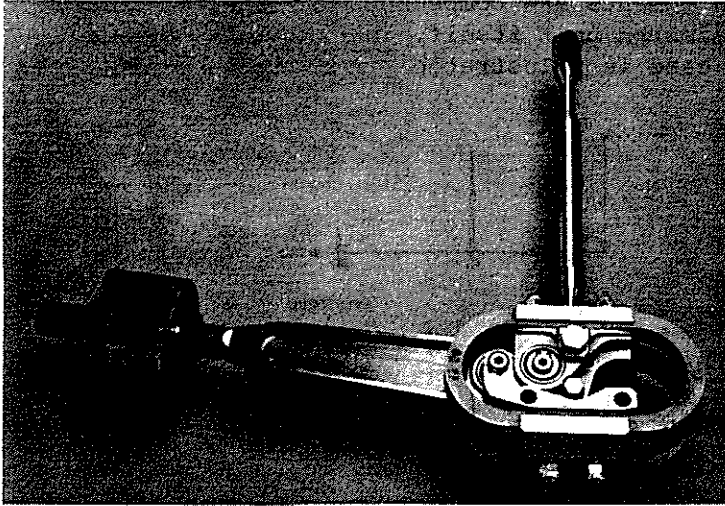


Figure 4: Construction design and schematic view of the antiresonance force isolator with mechanical pendulum

Two parallel GFRP ring-type springs serve as isolator spring. To connect the pendulum bar with the fuselage side and the gearbox side mountings of the isolator spring respectively, BARRY elastomeric bearings are used. The following requirements had to be met:

- very high radial stiffness of the bearing
- low torsional stiffness of the bearing
- very low lossfactor of the elastomeric material .

The elastomeric bearings have been found to be the most suitable out of several pendulum bearings tested. The main properties of the considered pendulum bearings are summarized in Table 1.

type of bearing	advantages	disadvantages
sliding bearings (several diameters)	high radial loading capacity	very low isolation effect, high wear, severe noise generation
needle bearings (two rows; 1 mm needle- ϕ)	high radial loading capacity, moderate isolation effect	relative high wear, severe noise generation
BENDIX-flexural pivots	very good isolation efficiency, nearly noiseless	too small radial loading capacity, too small radial stiffness
BARRY-elastomeric bearings	good isolation efficiency nearly noiseless, high radial loading capacity	relative high torsional stiffness

Table 1: Advantages and disadvantages of the pendulum bearings tested

As connecting elements between isolator and gearbox, pinned joints with flexible segments (quasi-hinges) at both ends, are used.

To predict theoretically the influences of the different construction parameters and component properties on the operating capability of the isolator with mechanical force generator, the isolator is substituted by the dynamic system shown in Fig. 5. The movements of the rotor-transmission mass M_R , fuselage mass M_F , and pendulum mass M_D are described by

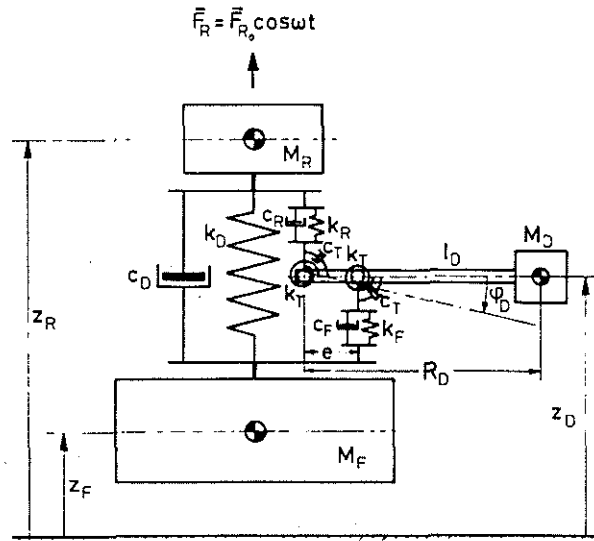


Figure 5: Theoretical dynamic model for the antiresonance force isolator with mechanical pendulum

the absolute coordinates z_R , z_F , and z_D . Additionally, the auxiliary angle coordinate ϕ_D is introduced. The pendulum bearings are simulated radially by the spring-damper combination c_R , k_R and c_F , k_F respectively, and torsionally by the torsion spring - torsion damper combination c_T , k_T . The equations of motion for this equivalent dynamic system are:

$$[M] \{\ddot{z}\} + [C] \{\dot{z}\} + [K] \{z\} = \{F_R\} \quad (1)$$

$$\text{with } \{z\} = \begin{Bmatrix} z_R \\ z_F \\ z_D \\ \phi_D \end{Bmatrix} \quad \text{and } \{F_R\} = \begin{Bmatrix} F_R \\ 0 \\ 0 \\ 0 \end{Bmatrix} .$$

The inertia matrix $[M]$, the damping matrix $[C]$ and the stiffness matrix $[K]$ are presented at full length in Appendix A. By disregarding the damping, the tuning equation results from Eq. 1 for $z_F = 0$:

$$M_D = \frac{k_{\text{tot}} [k_T^* (k_F + k_R) + k_F k_R] - \omega_a^2 I_D^* [k_D (k_F + k_R) + k_F k_R]}{\omega_a^2 \{k_D [k_T^* - \omega_a^2 I_D^* + k_F (Q_R - 1)^2 + k_R Q_R^2] + k_F k_R Q_R (Q_R - 1)\}} , \quad (2)$$

$$\text{with } k_{\text{tot}} = k_D + \frac{1}{\frac{1}{k_F} + \frac{1}{k_R} + \frac{1}{k_T^*}}$$

For pendulum bearings of infinite radial stiffness ($k_F, k_R \rightarrow \infty$) and very low torsional stiffness ($k_T \rightarrow 0$) and ignoring the intrinsic inertia moment of the pendulum bar ($I_D = 0$), this relation can be reduced to the well known tuning equation [1]

$$M_D = \frac{k_D}{\omega_a^2 Q_R (Q_R - 1)} \quad (3)$$

5. Isolator with hydraulic force generator

The antiresonance isolator supplied with a passive hydraulic force generator is in principle similar to the isolator with mechanically driven force generator, described in the preceding section. Fundamentally, this kind of isolator is also a parallel connection of a spring and a pendulum possessing, however, an hydraulic transmission. The hydraulic force generator essentially consists of two metal bellows and an additional spring. The bellows form a self-contained unit which is completely filled with a low viscosity fluid. To minimize flow losses, it is necessary to avoid any sharp edge within the bellows system. The pendulum weight, which is fastened to the free end of the smaller (secondary) bellows, is supported by suitable linear bearings. For fine tuning, it consists of several disks. The additional spring pressurizes the fluid in the bellows system. The basic design of the isolator with hydraulic force generator is shown in Fig. 6. For comparison, the corresponding model with a mechanical pendulum is presented.

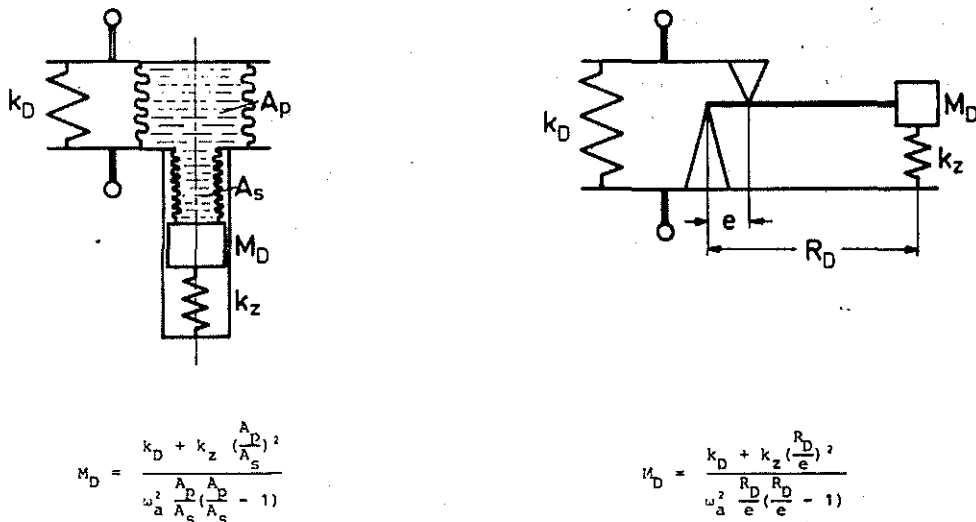


Figure 6: Basic design of the passive antiresonance isolator with hydraulic force generator in comparison with the corresponding model with mechanical pendulum

For both diagrammatic sketches the characteristic tuning equation is indicated, where the following assumptions have been made:

- 1) The pendulum of the mechanical force generator is regarded as a mathematical pendulum.
- 2) The liquid volume of the hydraulic force generator is constant.

The method of operation is that the stroke of the primary bellows caused by a periodical movement of the gearbox relative to the fuselage, generates an enlarged stroke of the secondary bellows and of the pendulum weight. The resultant inertia force produces a pressure change in the fluid which bears as a dynamic force upon the fuselage side and the gearbox side attachment points of the isolator. For the tuning frequency, these dynamic forces are in phase opposition to the isolator spring forces.

In Fig. 7 a construction model of the isolator with hydraulic force generator is illustrated. For better understanding, the schematic arrangement is additionally shown. This isolator is suitable for installation as a lateral isolator in the BK 117 helicopter. The primary bellows is a thick-walled type which also serves as isolator-gearbox spring, and as isolator-fuselage connecting hinge and as isolator-gearbox connecting hinge respectively.

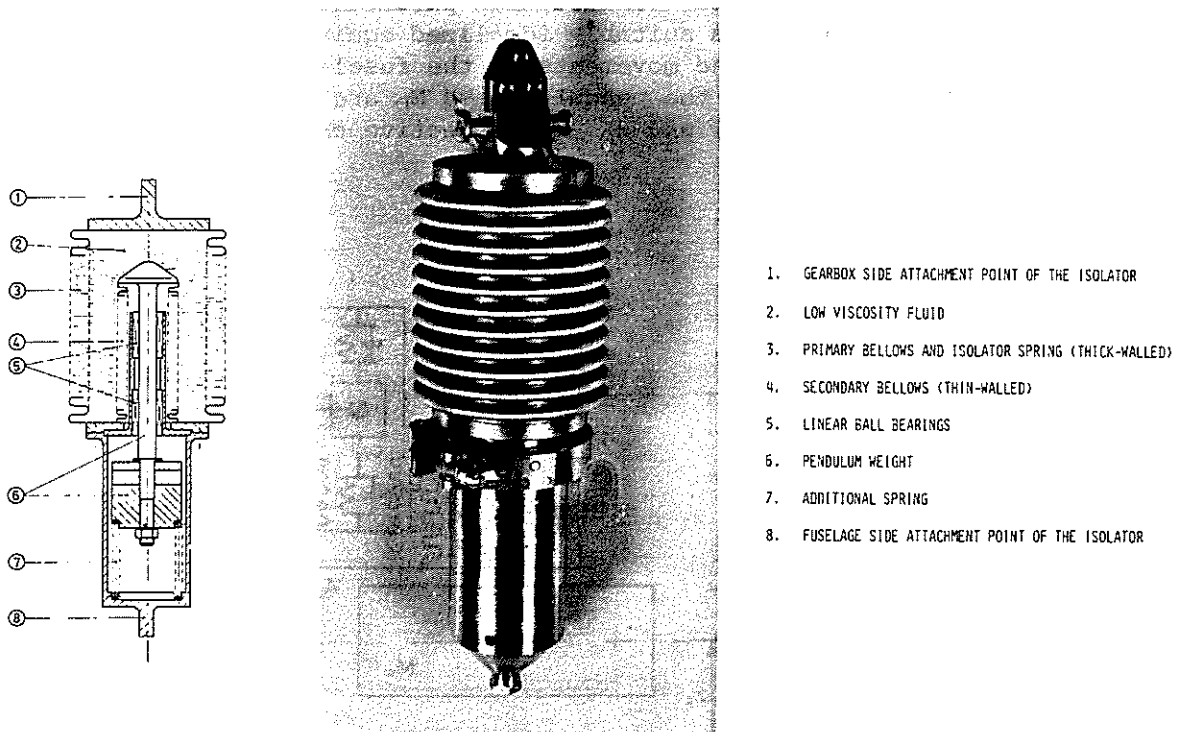


Figure 7: Construction design and schematic view of the antiresonance force isolator with hydraulic pendulum

The secondary bellows is thin-walled and allows high axial displacements. The pendulum weight is guided in the axial direction by two linear ball bearings. The main advantages of this isolator type are as follows:

- total symmetrical arrangement of isolator spring and force generator
- simple wear-resistant design
- use of only approved low-cost components
- only translational movements of the pendulum weight permitted
- heavily loaded pendulum bearings not required
- very low inherent damping of isolator spring and force generator
- very good linearity of the isolator springs
- small installation space
- low weight
- the force generator also allows relative displacements out of the isolator operating direction
- possibility for two-frequency isolation by simple addition of a second spring-mass system.

For the general theoretical understanding and for the study of the influences of the particular construction parameters on the operating quality of the isolator, a suitably idealized equivalent dynamical system is introduced (Fig. 8). The movements of the fuselage mass M_F , the rotor-transmission mass M_R , and the pendulum mass M_D are described by the absolute coordinates z_F , z_R , and z_D . The effective cross-sectional area of

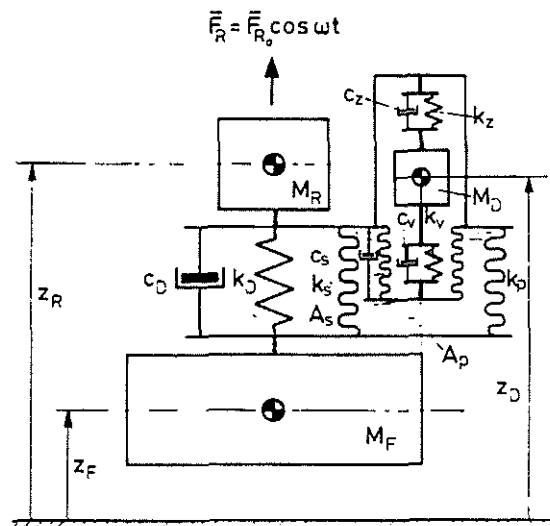


Figure 8: Theoretical dynamic model for the antiresonance force isolator with hydraulic pendulum

the outer bellows is A_p , of the inner bellows A_s . The spring-damper combination k_v , c_v simulates the volume stiffness of the bellows system which has a significant influence on the isolator efficiency. The corresponding

equations of motion in matrix notation are:

$$[M]\{\ddot{z}\} + [C]\{\dot{z}\} + [K]\{z\} = \{F_R\} \quad (4)$$

$$\text{with } \{z\} = \begin{Bmatrix} z_R \\ z_F \\ z_D \end{Bmatrix} \text{ and } \{F_R\} = \begin{Bmatrix} F_R \\ 0 \\ 0 \end{Bmatrix}$$

The inertia matrix [M], the damping matrix [C], and the stiffness matrix [K] are given in Appendix B.

Disregarding the damping, the equations of motion yield for $z_F = 0$ the tuning equation

$$M_D = \frac{k_{\text{tot}}(k_z + k_v)}{\omega_a^2 [k_D + k_p + k_s Q_A^2 + k_v Q_A (Q_A - 1)]} \quad (5)$$

$$\text{with } k_{\text{tot}} = k_D + k_p + Q_A^2 \left(k_s + \frac{k_z k_v}{k_z + k_v} \right).$$

Assuming that the fluid volume does not change during the cycle, i.e. for $k_v \rightarrow \infty$, Eq. (5) can be reduced to

$$M_D = \frac{k_{\text{tot}}}{\omega_a^2 Q_A (Q_A - 1)}, \quad (6)$$

$$\text{with } k_{\text{tot}} = k_D + k_p + Q_A^2 (k_s + k_z).$$

6. Experiments ¹⁾

The effectiveness of the presented force isolators is proved by use of an uniaxial functional model by which the free-free condition of the flying helicopter can be simulated in the vertical vibration direction (Fig. 9). The equivalent rotor-transmission mass is suspended on a very weak air spring. The equivalent fuselage mass is coupled to the rotor-transmission unit using the force isolator as connecting member. The rotor-transmission mass and fuselage mass are guided in the vertical direction by weak leaf-springs. The rotor-transmission unit is sinusoidally excited by an electrodynamic shaker which is positioned below the fuselage mass.

In quantifying the operating quality of the antiresonance isolation system, it is useful to compare the inertia force reacting on the fuselage mass $M_F \ddot{z}_F$ with the rotor excitation force F_R . Measuring equipment is provided for the on-line recording of amplitude and phase characteristics of this so-called fuselage-c.g. transmissibility.

¹⁾ The experiments have been performed in cooperation with the DFVLR Göttingen.

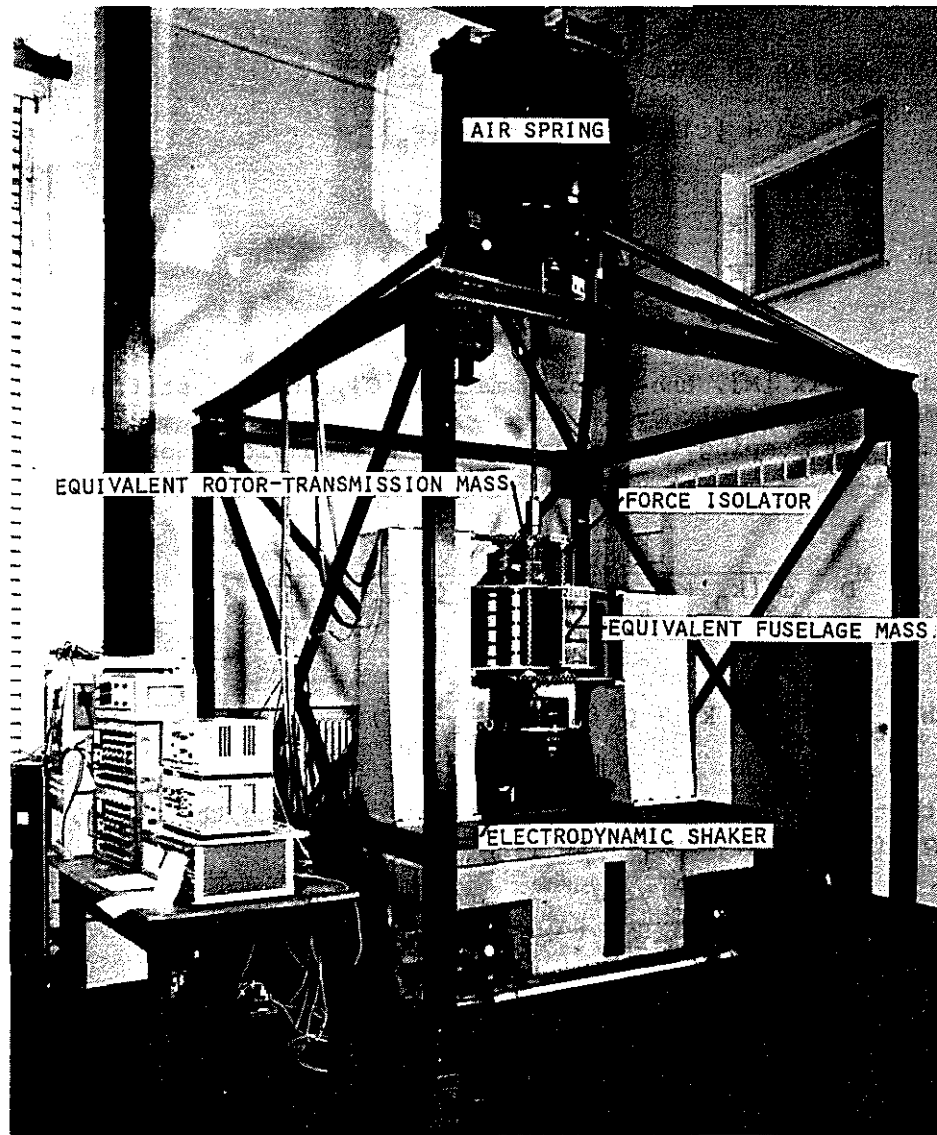


Figure 9: Total view of the uniaxial functional model for isolator test at the DFVLR Göttingen

7. Results

Both presented isolator types have been tested on the uniaxial functional model. In Figs. 10 and 11 the measured amplitude and phase characteristics of the fuselage-c.g. transmissibility are shown. The dotted curves are the corresponding theoretical results determined from Eqs. (1) and (4). In addition, the time history of the measuring values F_R , \ddot{z}_R , \ddot{z}_F , Δz , \ddot{z}_D and Δp respectively in the isolation case are represented in Figs. 12 and 13.

The main experimental data are summarized in Table 2. The numerical values used with the theory have been measured in separate experiments or taken from manufacturers specifications. Good agreement is achieved between theoretical and experimental results. In particular, with the hydraulic version, excellent isolation efficiency is obtained (better than 99%). The reason for this is the very low self-damping of the hydraulic isolator (about .2% referred to the weight of the rotor-transmission unit).

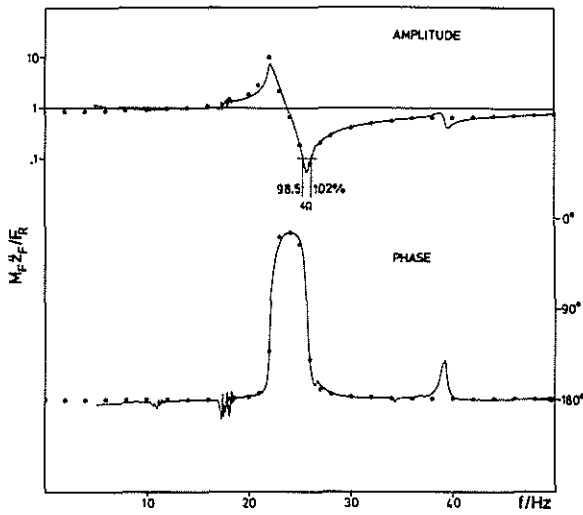


Fig. 10: Amplitude and phase characteristics of the fuselage-c.g. transmissibility for the antiresonance force isolator with mechanical pendulum

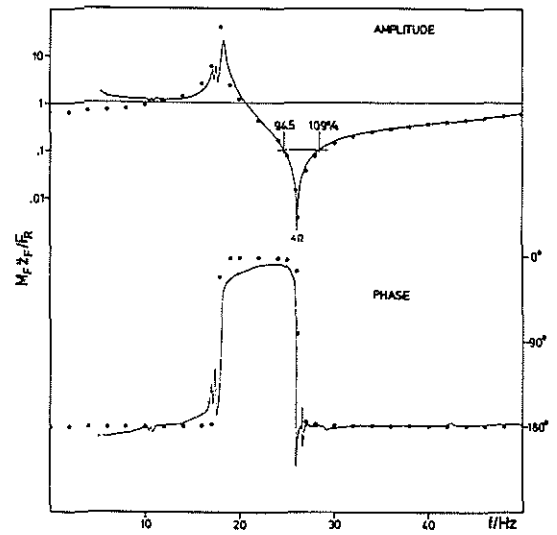


Fig. 11: Amplitude and phase characteristics of the fuselage-c.g. transmissibility for the passive antiresonance isolator with hydraulic force generator

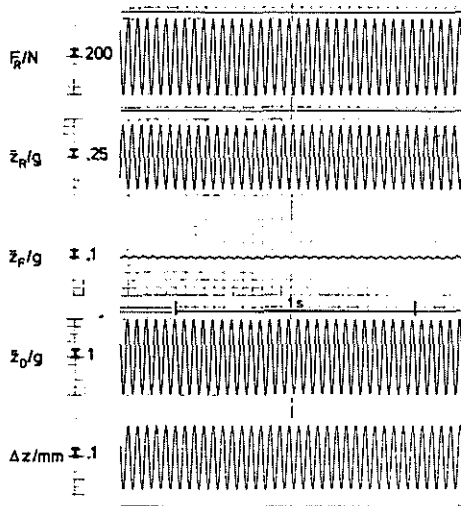


Fig. 12: Time history of the characteristic measuring values in the isolation case for the antiresonance force isolator with mechanical pendulum

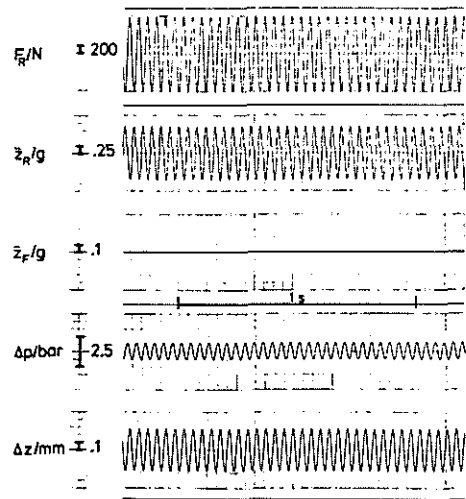


Fig. 13: Time history of the characteristic measuring values in the isolation case for the passive antiresonance isolator with hydraulic force generator

isolator with	mechanical force generator	hydraulic force generator
M_F/kg	650	300
M_R/kg	135	135
M_D/kg	2	1.27
I_D/kgm^2	.03	-
$R_D/e, A_p/A_s$	9.6	7.3
k_{tot}/Nm^{-1}	6.3×10^6	1.7×10^6
ζ_{tot}	.025	< .005
total isolator weight / kg	6.5	4.5
fluid in the bellows system	-	water-alcohol mixture

Table 2: Main experimental data of the uniaxial functional model

8. Concluding remarks

Both types of antiresonance force isolators presented in this paper have demonstrated their isolation efficiency. The theoretically predicted results have been confirmed by the experiments. For the conventional isolator type elastomeric pivots have proved to be the most suitable pendulum bearings. In particular with the novel hydraulic isolator, an excellent degree of isolation is obtained. Quasi-static and dynamic life tests performed with the first prototype of the hydraulic version predict a service life of at least 2000 hours. A similarly designed vertical force isolator is being manufactured.

Ground and flight tests with a four-axes isolation system consisting of mechanical and hydraulic isolator elements respectively will be performed on the BK 117 helicopter.

Acknowledgment

The author wish to acknowledge support for the research by the Bundesministerium für Forschung und Technologie (BMFT).

References

1. W.G. Flannelly The Dynamic Anti-Resonant Vibration Isolator.
Presented at the 22nd Annual AHS National Forum,
Washington, D.C., May 1966

2. A.D. Rita,
J.H. McGarvey,
R. Jones Helicopter Rotor Isolation Evaluation utilizing
the Dynamic Antiresonant Vibration Isolator.
Presented at the 32nd Annual AHS National Forum,
Washington, D.C., May 1976

3. R.A. Desjardins,
W.E. Hooper Rotor Isolation of the Hingeless Rotor BO 105
and YUH-61 Helicopters.
Presented at the 2nd European Rotorcraft and
Powered Lift Aircraft Forum, Bückebug, FRG,
September 1976

4. R.A. Desjardins,
W.E. Hooper Antiresonant Rotor Isolation for Vibration
Reduction.
Presented at the 34th Annual AHS National Forum,
Washington, D.C., May 1978

5. D.R. Halwes LIVE-Liquid Inertia Vibration Eliminator.
Presented at the 36th Annual AHS Forum,
Washington, D.C., May 1980

Appendix A

$$[M] = \begin{bmatrix} M_R & & & \\ & M_F & & \\ & & M_D & \\ & & & I_D \end{bmatrix}$$

$$[C] = \begin{bmatrix} c_D + c_R & -c_D & -c_R & -c_{R_D}^R \\ -c_D & c_D + c_F & -c_F & -c_F(R_D - e) \\ -c_R & -c_F & c_F + c_R & c_F(R_D - e) + c_{R_D}^R \\ -c_{R_D}^R & -c_F(R_D - e) & c_F(R_D - e) + c_{R_D}^R & c_F(R_D - e)^2 + c_{R_D}^R + 2c_T \end{bmatrix}$$

$$[K] = \begin{bmatrix} k_D + k_R & -k_D & -k_R & -k_{R_D}^R \\ -k_D & k_D + k_F & -k_F & -k_F(R_D - e) \\ -k_R & -k_F & k_F + k_R & k_F(R_D - e) + k_{R_D}^R \\ -k_{R_D}^R & -k_F(R_D - e) & k_F(R_D - e) + k_{R_D}^R & k_F(R_D - e)^2 + k_{R_D}^R + 2k_T \end{bmatrix}$$

Appendix B

$$[M] = \begin{bmatrix} M_R & & \\ & M_F & \\ & & M_D \end{bmatrix}$$

$$[C] = \begin{bmatrix} c_D + c_Z + c_S Q_A^2 + c_V (Q_A - 1)^2 & -c_D - c_S Q_A^2 - c_V Q_A (Q_A - 1) & -c_Z + c_V (Q_A - 1) \\ -c_D - c_S Q_A^2 - c_V Q_A (Q_A - 1) & c_D + (c_S + c_V) Q_A^2 & -c_V Q_A \\ -c_Z + c_V (Q_A - 1) & -c_V Q_A & c_Z + c_V \end{bmatrix}$$

$$[K] = \begin{bmatrix} k_D + k_P + k_Z + k_S Q_A^2 + k_V (Q_A - 1)^2 & -k_D - k_P - k_S Q_A^2 - k_V Q_A (Q_A - 1) & -k_Z + k_V (Q_A - 1) \\ -k_D - k_P - k_S Q_A^2 - k_V Q_A (Q_A - 1) & k_D + k_P + (k_S + k_V) Q_A^2 & -k_V Q_A \\ -k_Z + k_V (Q_A - 1) & -k_V Q_A & k_Z + k_V \end{bmatrix}$$